

See discussions, stats, and author profiles for this publication at: <https://www.researchgate.net/publication/230562861>

n-Type Semiconducting Polymer Fibers

ARTICLE in ACS MACRO LETTERS · MARCH 2012

Impact Factor: 5.76 · DOI: 10.1021/mz200208b

CITATIONS

12

READS

60

6 AUTHORS, INCLUDING:



[Eleonora Valeria Canesi](#)

Istituto Italiano di Tecnologia

29 PUBLICATIONS 211 CITATIONS

[SEE PROFILE](#)



[Alessandro Luzio](#)

Istituto Italiano di Tecnologia

21 PUBLICATIONS 169 CITATIONS

[SEE PROFILE](#)



[Andrea Bianco](#)

National Institute of Astrophysics

91 PUBLICATIONS 676 CITATIONS

[SEE PROFILE](#)



[Mario Caironi](#)

Istituto Italiano di Tecnologia

87 PUBLICATIONS 1,674 CITATIONS

[SEE PROFILE](#)

n-Type Semiconducting Polymer Fibers

Eleonora V. Canesi,[†] Alessandro Luzio,[†] Beatrice Saglio,[‡] Andrea Bianco,[§] Mario Caironi,^{*,†} and Chiara Bertarelli^{*,‡,†}

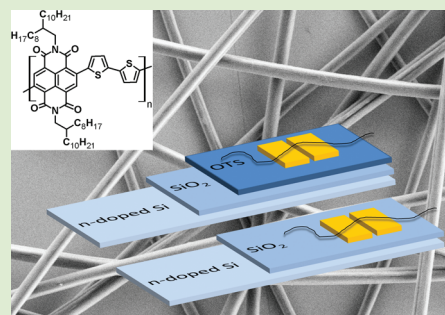
[‡]Dipartimento di Chimica, Materiali e Ing. Chimica "G. Natta", Politecnico di Milano, Piazza L. Da Vinci 32, 20133 Milano, Italy

[†]Center for Nano Science and Technology @PoliMi, Istituto Italiano di Tecnologia, Via Pascoli 70/3, 20133 Milano, Italy

[§]INAF - Osservatorio Astronomico di Brera, Via Bianchi 46, 23807 Merate, Italy

Supporting Information

ABSTRACT: Defect-free bicomponent fibers of poly{[*N,N'*-bis(2-octyl-dodecyl)-naphthalene-1,4,5,8-bis(dicarboximide)-2,6-diyl]-*alt*-5,5'-(2,2'-bithiophene)} / poly(ethyleneoxide) P(NDI2OD-T2)/PEO are fabricated by means of electrospinning and rinsed with a selective solvent to afford pure P(NDI2OD-T2) while maintaining a fibrous morphology. The elongation strength applied on the spun jet by the high electrical field induces a preferential orientation of polymer chains. An electron mobility analogous to the best obtained with a thin film-based device is achieved in single fiber transistors, and the results are unaffected by the dielectric surface treatment.



Solution processed semiconducting nano- and microwires are of great interest, since they combine unique dimensionality and functional properties with ease of fabrication.¹ In particular, electrospun fibers of conjugated polymers have received an increasing attention in the last years, thanks to the simplicity and versatility of this processing technique.^{2,3} Polymers with a conducting behavior, such as polypyrrole,^{4–6} polyaniline,⁷ or poly(ethylenedioxythiophene),⁸ have been processed by means of electrospinning, and applications in fields ranging from gas sensors^{9,10} to electromagnetic shielding^{11,12} have been demonstrated.

Moreover, some examples of electrospun fibers of conjugated polymers showing a *p*-type semiconducting behavior have been reported and tested in transistor devices.^{13–17} To afford the demonstration of advanced electronic functionalities, electron transporting polymeric fibers, the complementary part which would enable fiber-based robust logic circuits, are required as well. To date, only *n*-channel wires produced by self-assembly have been reported in the literature,^{18,19} whereas, to the best of our knowledge, no *n*-type polymer fiber has been electrospun yet, mainly due to the limited availability of environmentally stable and easily processable *n*-type conjugated polymers.

In this communication we fill this gap by demonstrating defect-free electrospun microfibers of poly{[*N,N'*-bis(2-octyl-dodecyl)-naphthalene-1,4,5,8-bis(dicarboximide)-2,6-diyl]-*alt*-5,5'-(2,2'-bithiophene)} (P(NDI2OD-T2))^{20,21}, a soluble and air-stable *n*-channel polymeric semiconductor, and by successfully applying them in single fiber-based field-effect transistors (FETs). When in the form of a thin film, P(NDI2OD-T2) shows the highest field-effect electron mobility reported so far for a polymeric semiconductor, and it is currently the subject of extensive studies aimed at clarifying its charge transport properties.^{22–27} Interestingly, here we clearly evidence a

lower sensitivity of single-fiber transistors to the dielectric/semiconductor interface chemistry with respect to thin film devices while showing comparable or better performances.

With respect to traditional polymeric materials, conjugated polymers are characterized by a more rigid backbone, which limits the number of entanglements that assist the fibers formation during electrospinning, preventing the jet breaking under the elongation strength.²⁸ Accordingly, several strategies have been proposed,^{29,30} including coaxial spinning,^{31,32} polymerization on as-spun fibers surface,^{5,8,33} or the addition of a second polymer to the feed solution, which supports the fibers formation.^{34–36} A proper choice of the supporting polymer would then allow its selective rinsing to afford fibers of the pure conjugated polymer.^{8,37}

Following the last method, poly(ethyleneoxide) (PEO) has been blended, as supporting polymer, with P(NDI2OD-T2), with a quantity ranging from 30 to 50% in weight of the total amount of the two polymers. Processing parameters, namely solution concentration, applied voltage, and volume flow rate, have been varied to find the optimal conditions to obtain continuous, homogeneous P(NDI2OD-T2)/PEO fibers. Solution concentration (sum of the two polymers) lower than 5 w % was found to produce only polymer drops. Defect-free and smooth fibers with a circular-shaped cross section have been obtained with a concentration in the 5–7 w % range, a flow rate of 0.1–0.2 mL h^{−1} and a voltage of 23–30 kV. The variation of the experimental conditions within these ranges turned out to affect the deviation in fibers diameter but defects, such as beads

Received: December 6, 2011

Accepted: February 2, 2012

or porous structures, have never been obtained (see Supporting Information).

The best results were obtained by electrospinning solutions with a 5 w % concentration of a 70:30 w/w mixture of P(NDI2OD-T2)/PEO in chlorobenzene, at an applied voltage of 23 kV and at a flow rate of 0.1 mL h⁻¹ (Figure 1a). The

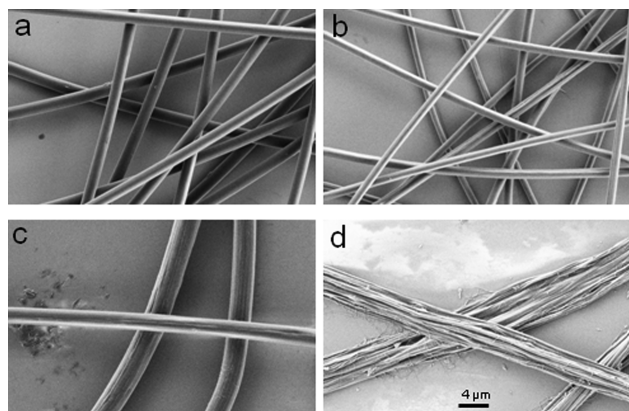


Figure 1. SEM images of P(NDI2OD-T2)/PEO fibers, obtained by applying a voltage of 23 kV, with a flow rate of 0.1 mL h⁻¹ from a solution 5 w % in chlorobenzene: the relative content of the two polymers is equal to (a) 70:30 w/w; (b) 70:30 w/w, upon rinsing with acetonitrile; (c) 50:50 w/w; and (d) 50:50 w/w, upon rinsing with acetonitrile.

average diameter of these fibers is 1.46 μm with a standard deviation of only 78 nm. The very narrow standard deviation, if compared with the average diameter, clearly evidences the homogeneity of the spun fibers and at the same time the stability of the spinning process. The possibility to control the fibers diameter distribution within a very limited dispersion is extremely relevant for applications in electronic devices.

By rinsing the sample with acetonitrile, PEO was selectively removed. It is noteworthy that fibers still appear continuous and homogeneous and their surface is slightly striped (Figure 1b). Removal of the supporting polymer is accompanied by the reduction of the average diameter of the fibers: the above cited sample undergoes a reduction from 1.46 to 1.18 μm, roughly consistent with the quantity of PEO in the blend.

The effectiveness of rinsing was confirmed by means of FT-IR spectroscopy: by analyzing a P(NDI2OD-T2)/PEO fibrous mat collected on a ZnSe disk (see Supporting Information, Figure S02), we clearly detect the main characteristic features of both of the two components, namely, the band around 1100 cm⁻¹, which is related to the C–O–C stretching of PEO, and bands in the region 1610–1720 cm⁻¹, which are peculiar of the conjugated polymer. The disappearance of the strong signal at 1100 cm⁻¹ shows the complete PEO removal upon rinsing with acetonitrile (Figure S03).

Starting from the initial 70:30 w/w, relative concentration of the two compounds into the blend was varied. The increase in PEO content in the feed solution was expected to further improve the fibers formation and to produce thinner fibers once they are rinsed, with the quantity of P(NDI2OD-T2) being smaller. We verified that continuous, homogeneous fibers can still be obtained with a ratio down to 50:50 w/w (P(NDI2OD-T2)/PEO) (Figure 1c); however, by washing with acetonitrile, the resulting fiber surface was strongly rough and a partial unraveling occurred (Figure 1d). For this reason,

the ratio 70:30 w/w was taken as the standard for the hereafter described investigations.

It has been demonstrated that a preferential orientation of polymer chains along the fiber axis can be triggered by the significant jet elongation during the electrospinning process.^{38,39} To ascertain this phenomenon in the present study, a mat of P(NDI2OD-T2) fibers aligned along a preferential uniaxial direction has been analyzed by polarized infrared spectroscopy, and a dichroic ratio different than 1 has been detected for some of the characteristic bands of P(NDI2OD-T2), namely 1705 and 1665 cm⁻¹. These results likely provide the first evidence of the preferential orientation of the polymer chains with respect to the fibers axis (Figure S04). Nevertheless, we were not able to definitively quantify the phenomenon (i.e. cos² θ), the direction of the transition moments of the normal modes of interest being not known. Additional measurements would be required to go into the matter.

To test the electrical properties of fibers of P(NDI2OD-T2) and how the fibrous morphology affects performance in electronics applications, FETs were fabricated where fibers constitute the semiconducting layer. These devices were compared to the correspondent P(NDI2OD-T2) thin-film based FETs. Here we adopted a bottom gate, bottom contacts (BGBC) architecture (Figure 2a) with SiO₂ as gate dielectric,

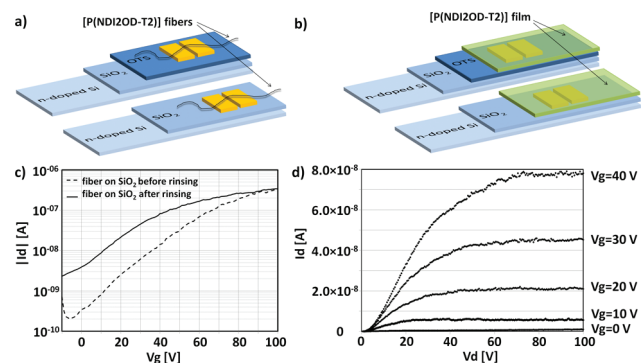


Figure 2. Schemes of the BGBC single-fiber (a) and thin-film (b) FETs on bare SiO₂; channels 20 μm long and 10000 μm wide gold source and drain electrodes were employed. (c) Plot of the transfer curves of a single-fiber device before (dashed line) and after (continuous line) the removal of the PEO; a drain voltage of 100 V was applied during the measurements; (d) output curves of a P(NDI2OD-T2)-only single-fiber transistor after rinsing with acetonitrile.

which greatly simplifies the fiber-based device fabrication. This architecture was previously reported not to be optimal for a thin-film P(NDI2OD-T2) device, although a mobility ~0.1 cm² V⁻¹ s⁻¹ could be obtained by functionalizing the interface with an octadecyltrichlorosilane (OTS) buffer layer.²³ We tested both the fibers and film based FETs with and without OTS functionalization. A contact angle of 110° was measured for the OTS treated SiO₂ substrates, compared to the ~50° of a bare substrate, thus proving the effectiveness of the silanization process.

In Figure 2c the transfer characteristic curves of P(NDI2OD-T2)/PEO and P(NDI2OD-T2)-only (upon rinsing with acetonitrile) single-fiber FETs on bare SiO₂ are reported. The output characteristics are shown in Figure 2d in the case of a single fiber device on bare SiO₂ upon rinsing.

To the best of our knowledge, this is the first report of *n*-channel field-effect behavior in a polymeric fiber-based FET. The field-effect mobility μ has been extracted by conservatively assuming that the channel width *W* coincides with the fiber diameter (see Supporting Information). Single-fiber FETs show a mobility in the saturation regime in the $0.05\text{--}0.09\text{ cm}^2\text{ V}^{-1}\text{ s}^{-1}$ range, both before and after PEO removal, both with and without OTS treatment. The measured μ values exactly correspond to those of the best thin film FETs on OTS we have realized ($\mu \approx 0.07\text{--}0.08\text{ cm}^2\text{ V}^{-1}\text{ s}^{-1}$), and very close to the best mobility reported in literature on a P(NDI2OD-T2) thin film, BGBC FET.²³ Moreover, single fiber FETs exhibit ON/OFF current ratio totally comparable to those of the thin film-based FETs (see Table S02).

Overall, the semiconducting fibers appear to be very little affected by their surroundings and especially by the chemistry of the dielectric/semiconductor interface. In fact, as a first interesting observation, both FETs with and without rinsing show similar μ , with only a reduced ON/OFF ratio and a shift of the current onset (details in the Supporting Information) upon rinsing. Therefore, insulating PEO molecules do not impede an efficient electron transport throughout the P-(NDI2OD-T2) phase along the whole fiber's length, likely due to phase separation.^{40–42} This is interesting because in similar experiences the presence of the supporting polymer has been found to negatively affect the charge transport mechanism into the electrospun fibers.^{13,15}

A second intriguing aspect regards the substantial insensitivity of single fiber FETs μ to surface treatment, at variance with thin-film FETs. The superposition of the transfer characteristic curves of the single fiber devices and of the thin-film devices, reported in Figure 3, enables the comparison

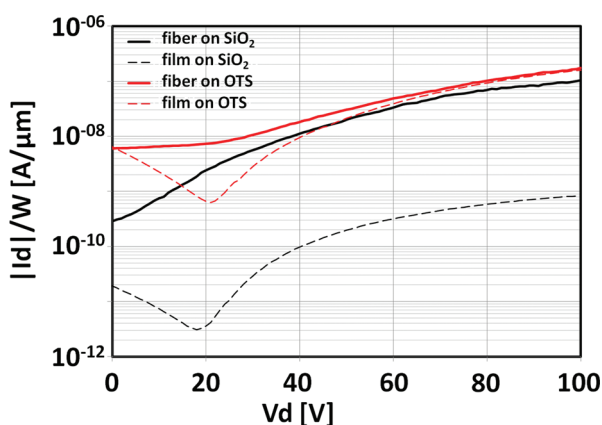


Figure 3. Transfer curves of single fiber (continuous lines) and thin film (dashed lines) P(NDI2OD-T2) FETs; the characteristics of devices on both bare SiO₂ (black lines) and OTS treated dielectric layers (red lines) are reported; a drain voltage of 100 V was applied during all the measurements; in the plot, drain current values are normalized to the channel width, which in the case of the fiber was conservatively assumed to be equal to its diameter.

of their field-effect behaviors. Currents were normalized to *W*, and also in this case, we conservatively assumed that for the fibers it corresponds with their diameter.

Thin film FET performances are negatively affected by the bare SiO₂ substrate ($\mu \sim 5 \times 10^{-4}$), whereas a strong improvement is observed when the OTS buffer layer is employed ($\mu \sim 0.07\text{--}0.08$), consistently with literature

data.^{21,23} On the contrary, single-fiber FETs did not show any change in performances induced by modification of the interface with the dielectric, the fibers on bare SiO₂ providing almost the same currents as the ones measured on OTS. This might be due to the limited contact area between the fiber and the dielectric surface (see Supporting Information) and their limited interaction. It is worth noting that a strong underestimation of the mobility values as calculated in this work would derive from this hypothesis, meaning that the fiber performances are actually much higher than those here reported. It should be taken into account that, contrary to the film formation, the spun jet of P(NDI2OD-T2) solidifies into a fiber before getting into contact with the dielectric surface. The fiber surface is therefore formed independently of the particular dielectric, providing another possible factor for the observed fiber FETs insensitivity to the semiconductor/interface chemistry. This represents a relevant advantage as it shows that these semiconducting fibers have a potential for easy integration in a variety of applications.

In conclusion, P(NDI2OD-T2) has been successfully electrospun providing homogeneous defect-free fibers with a preferential orientation of P(NDI2OD-T2) polymer chains along the fiber axis. The fibers performance on a BCBG FET device is the same or even better than that of an analogous device based on a thin film of P(NDI2OD-T2) and is characterized by an interesting insensitivity to the nature of the interface with the dielectric. Besides providing indications on the parameters affecting charge transport mechanism in a high-mobility *n*-type polymer, our results are important for the further development of advanced electronics applications in smart textiles.

EXPERIMENTAL METHODS

PEO ($M_w = 4000000$, Sigma-Aldrich) and P(NDI2OD-T2) (Polyera ActivInk N2200, $M_w = 100000\text{--}150000$) were dissolved in chlorobenzene (Sigma-Aldrich) before being transferred to the electrospinning setup (KDS Scientific infusion pump, Spellman high voltage power supply). Field emission SEM Zeiss SUPRA 40 was used for scanning electron microscopy, Thermo Nicolet Nexus for FT-IR spectroscopy. The base FET structures (*n*-doped silicon gate, 230 nm thick SiO₂ gate dielectric, and 30 nm thick source and drain Au electrodes, with 10 nm thick high work function ITO adhesion layer) were purchased from Fraunhofer IPMS. OFETs electrical measurements were performed under nitrogen atmosphere by employing a probe station connected to an Agilent B1500.

ASSOCIATED CONTENT

Supporting Information

Experimental methods, additional data about the electrospinning parameters and the electrical characterization of single fiber-based transistors and infrared spectra are reported. This material is available free of charge via the Internet at <http://pubs.acs.org>.

AUTHOR INFORMATION

Corresponding Author

*E-mail: chiara.bertarelli@polimi.it (C.B.); mario.caironi@iit.it (M.C.). Tel.: +39 02 2399 3224 (C.B.); +39 02 2399 9875 (M.C.).

Notes

The authors declare no competing financial interest.

ACKNOWLEDGMENTS

The authors are thankful to D. Natali for helpful discussions. M.C. acknowledges the financial support of the European Union under the Marie Curie Career Integration Fellowship "IPPIA". C. B. and E.V.C. acknowledge Fondazione Cariplo that partly supports this work through the project "MATHYS" (Grant No. ref.2009/2527).

REFERENCES

- (1) Kim, F. S.; Ren, G. Q.; Jenekhe, S. A. *Chem. Mater.* **2011**, *23*, 682–732.
- (2) Greiner, A.; Wendorff, J. H. *Angew. Chem., Int. Ed.* **2007**, *46*, 5670–5703.
- (3) Li, D.; Xia, Y. *Adv. Mater.* **2004**, *16*, 1151–1170.
- (4) Ji, L.; Yao, Y.; Toprakci, O.; Lin, Z.; Liang, Y.; Shi, Q.; Medford, A. J.; Millns, C. R.; Zhang, X. *J. Power Sources* **2010**, *195*, 2050–2056.
- (5) Granato, F.; Bianco, A.; Bertarelli, C.; Zerbi, G. *Macromol. Rapid Commun.* **2009**, *30*, 453–458.
- (6) Chronakis, I. S.; Grapenson, S.; Jakob, A. *Polymer* **2006**, *47*, 1597–1603.
- (7) Norris, I. D.; Shaker, M. M.; Ko, F. K.; MacDiarmid, A. G. *Synth. Met.* **2000**, *114*, 109–114.
- (8) Laforgue, A.; Robitaille, L. *Macromolecules* **2010**, *43*, 4194–4200.
- (9) Liu, H.; Kameoka, J.; Czaplewski, D. A.; Craighead, H. G. *Nano Lett.* **2004**, *4*, 671–675.
- (10) Wang, Y.; Jia, W.; Strout, T.; Schempf, A.; Zhang, H.; Li, B.; Cui, J.; Lei, Y. *Electroanalysis* **2009**, *21*, 1432–1438.
- (11) Saini, P.; Choudhary, V.; Singh, B. P.; Mathur, R. B.; Dhawan, S. K. *Mater. Chem. Phys.* **2009**, *113*, 919–926.
- (12) Kaynak, A.; Håkansson, E.; Amiet, A. *Synth. Met.* **2009**, *159*, 1373–1380.
- (13) Pinto, N. J.; Johnson, A. T.; MacDiarmid, A. G.; Mueller, C. H.; Theofylaktos, N.; Robinson, D. C.; Miranda, F. A. *Appl. Phys. Lett.* **2003**, *83*, 4244–4246.
- (14) Liu, H. Q.; Reccius, C. H.; Craighead, H. G. *Appl. Phys. Lett.* **2005**, *87*, 253106.
- (15) Lee, S.; Moon, G. D.; Jeong, U. J. *Mater. Chem.* **2009**, *19*, 743–748.
- (16) Tu, D. Y.; Pagliara, S.; Camposeo, A.; Persano, L.; Cingolani, R.; Pisignano, D. *Nanoscale* **2010**, *2*, 2217–2222.
- (17) Babel, A.; Li, D.; Xia, Y. N.; Jenekhe, S. A. *Macromolecules* **2005**, *38*, 4705–4711.
- (18) Brisenio, A. L.; Mannsfeld, S. C. B.; Shamberger, P. J.; Ohuchi, F. S.; Bao, Z. N.; Jenekhe, S. A.; Xia, Y. N. *Chem. Mater.* **2008**, *20*, 4712–4719.
- (19) Oh, J. H.; Lee, H. W.; Mannsfeld, S.; Stoltenberg, R. M.; Jung, E.; Jin, Y. W.; Kim, J. M.; Yoo, J.-B.; Bao, Z. *Proc. Natl. Acad. Sci. U.S.A.* **2009**, *106*, 6065–6070.
- (20) Yan, H.; Chen, Z.; Zheng, Y.; Newman, C.; Quinn, J. R.; Dotz, F.; Kastler, M.; Facchetti, A. *Nature* **2009**, *457*, 679–686.
- (21) Chen, Z.; Zheng, Y.; Yan, H.; Facchetti, A. *J. Am. Chem. Soc.* **2009**, *131*, 8–9.
- (22) Caironi, M.; Bird, M.; Fazzi, D.; Chen, Z.; Di Pietro, R.; Newman, C.; Facchetti, A.; Sirringhaus, H. *Adv. Funct. Mater.* **2011**, *21*, 3371–3381.
- (23) Rivnay, J.; Steyrleuthner, R.; Jimison, L. H.; Casadei, A.; Chen, Z.; Toney, M. F.; Facchetti, A.; Neher, D.; Salleo, A. *Macromolecules* **2011**, *44*, 5246–5255.
- (24) Rivnay, J.; Toney, M. F.; Zheng, Y.; Kauvar, I. V.; Chen, Z.; Wagner, V.; Facchetti, A.; Salleo, A. *Adv. Mater.* **2010**, *22*, 4359–4363.
- (25) Schuettfort, T.; Huettner, S.; Lilliu, S.; Macdonald, J. E.; Thomsen, L.; McNeill, C. R. *Macromolecules* **2011**, *44*, 1530–1539.
- (26) Sciascia, C.; Martino, N.; Schuettfort, T.; Watts, B.; Grancini, G.; Antognazza, M. R.; Zavelani-Rossi, M.; McNeill, C. R.; Caironi, M. *Adv. Mater.* **2011**, *23*, 5086–5090.
- (27) Fazzi, D.; Caironi, M.; Castiglioni, C. *J. Am. Chem. Soc.* **2011**, *133*, 19056–19059.
- (28) Shenoy, S. L.; Bates, W. D.; Frisch, H. L.; Wnek, G. E. *Polymer* **2005**, *46*, 3372–3384.
- (29) Chan, K. H. K.; Yamao, T.; Kotaki, M.; Hotta, S. *Synth. Met.* **2010**, *160*, 2587–2595.
- (30) Di Benedetto, F.; Camposeo, A.; Pagliara, S.; Mele, E.; Persano, L.; Stabile, R.; Cingolani, R.; Pisignano, D. *Nat. Nanotechnol.* **2008**, *3*, 614–619.
- (31) Li, D.; Babel, A.; Jenekhe, S. A.; Xia, Y. N. *Adv. Mater.* **2004**, *16*, 2062–2066.
- (32) Zhao, Q.; Xin, Y.; Huang, Z. H.; Liu, S. D.; Yang, C. H.; Li, Y. F. *Polymer* **2007**, *48*, 4311–4315.
- (33) Granato, F.; Scampicchio, M.; Bianco, A.; Mannino, S.; Bertarelli, C.; Zerbi, G. *Electroanalysis* **2008**, *20*, 1374–1377.
- (34) Laforgue, A.; Robitaille, L. *Synth. Met.* **2008**, *158*, 577–584.
- (35) Vohra, V.; Calzaferri, G.; Destri, S.; Pasini, M.; Porzio, W.; Botta, C. *ACS Nano* **2010**, *4*, 1409–1416.
- (36) Neubert, S.; Pliszka, D.; Thavasi, V.; Wintermantel, E.; Ramakrishna, S. *Mater. Sci. Eng., B* **2011**, *176*, 640–646.
- (37) Bianco, A.; Bertarelli, C.; Frisk, S.; Rabolt, J. F.; Gallazzi, M. C.; Zerbi, G. *Synth. Met.* **2007**, *157*, 276–281.
- (38) Fennessey, S. F.; Farris, R. J. *Polymer* **2004**, *45*, 4217–4225.
- (39) Bianco, A.; Iardino, G.; Manuelli, A.; Bertarelli, C.; Zerbi, G. *ChemPhysChem* **2007**, *8*, 510–514.
- (40) Lee, W. H.; Lim, J. A.; Kwak, D.; Cho, J. H.; Lee, H. S.; Choi, H. H.; Cho, K. *Adv. Mater.* **2009**, *21*, 4243–4248.
- (41) Madec, M. B.; Crouch, D.; Llorente, G. R.; Whittle, T. J.; Geoghegan, M.; Yeates, S. G. *J. Mater. Chem.* **2008**, *18*, 3230–3236.
- (42) Hamilton, R.; Smith, J.; Ogier, S.; Heeney, M.; Anthony, J. E.; McCulloch, I.; Veres, J.; Bradley, D. D. C.; Anthopoulos, T. D. *Adv. Mater.* **2009**, *21*, 1166–1171.